LIMNOLOGY and OCEANOGRAPHY

ASLO

Limnol. Oceanogr. 9999, 2025, 1–16

doi: 10.1002/lno.70023

RESEARCH ARTICLE

Gross oxygen production and microbial community respiration in the oligotrophic ocean

Sara Ferrón,[1*] **Karin M. Björkman**,[1] **Matthew J. Church**,[2] **David M. Karl**[1]

[1]Daniel K. Inouye Center for Microbial Oceanography: Research and Education, Department of Oceanography, School of Ocean and Earth Science and Technology, University of Hawai'i at Mānoa, Honolulu, Hawaii, USA; [2]Flathead Lake Biological Station, University of Montana, Polson, Montana, USA

Abstract

Uncertainties in the temporal and spatial patterns of marine primary production and respiration limit our understanding of the ocean carbon (C) cycle and our ability to predict its response to environmental changes. Here we present a comprehensive time-series analysis of plankton metabolism at the Hawaii Ocean Time-series program site, Station ALOHA, in the North Pacific Subtropical Gyre. Vertical profiles of gross oxygen production (GOP) and community respiration (CR) were quantified using the ^{18}O-labeled water method together with net changes in O_2 to Ar ratios during dawn to dusk in situ incubations. Rates of ^{14}C-bicarbonate assimilation (^{14}C-based primary production [^{14}C-PP]) were also determined concurrently. During the observational period (April 2015 to July 2020), euphotic zone depth-integrated (0–125 m) GOP and ^{14}C-PP ranged from 35 to 134 mmol O_2 m^{-2} d^{-1} and 18 to 75 mmol C m^{-2} d^{-1}, respectively, while CR ranged from 37 to 187 mmol O_2 m^{-2} d^{-1}. All biological rates varied with depth and season, with seasonality most pronounced in the lower portion of the euphotic zone (75–125 m). The mean annual ratio of GOP to ^{14}C-PP was 1.7 ± 0.1 mol O_2 (mol C)$^{-1}$. While previous studies have reported convergence of GOP and ^{14}C-PP with depth, we find a less pronounced vertical decline in the GOP to ^{14}C-PP ratios, with GOP exceeding ^{14}C-PP by 50% or more in the lower euphotic zone. Variability in CR was higher than for GOP, driving most of the variability in the balance between the two.

The reduction of carbon dioxide to organic matter through phytoplankton oxygenic photosynthesis is the main source of organic C and energy for heterotrophs in oceanic ecosystems (Karl 2014), accounting for approximately half of the primary production in the biosphere (Field et al. 1998). Phytoplankton primary production supports higher trophic levels (e.g., fisheries) and fuels the oceanic biological C pump, a process fundamental to the global C cycle, where organic and inorganic C are transported from the well-lit surface waters to the deep ocean. Respiration of organic matter regenerates nutrients needed for primary production and limits the organic C available for export to deeper layers. Understanding how primary production and respiration change in response to environmental variability is key to constraining the global C cycle and improving our ability to predict how the biological C pump will respond to climate change (Karl et al. 2003).

Accurate estimation of plankton metabolic rates is a great challenge for oceanographers, given a lack of standardization in how these processes are measured (IOCCG 2022). Field techniques to quantify photosynthetic rates range from measurements of gross or net O_2 production to measurements of net C accumulation (Church et al. 2019), whereas respiration is most often measured as O_2 consumption in the dark (Robinson and Williams 2005). One approach to constrain the uncertainty of primary production and respiration measurements is to compare different methods (Laws et al. 1984), which itself is challenging because different methods often measure different processes (e.g., gross vs. net primary production), in different units (e.g., C vs. O_2), and over different time

*Correspondence: sferron@hawaii.edu

Associate editor: Bingzhang Chen

Data Availability Statement: Rate measurements presented here are in the Zenodo data repository (https://doi.org/10.5281/zenodo.8388194) and will also be available at the Simons Collaborative Marine Atlas Project (https://simonscmap.com/). Data from the HOT program are available at https://hahana.soest.hawaii.edu/hot/hot-dogs/.

and spatial scales (e.g., incubation measurements vs. non-incubation mass balance estimates via chemical tracers). However, these comparisons can be useful not only for estimating the uncertainty of the measurements but also for understanding physiological and ecological processes that introduce variability in primary production and respiration.

At Station ALOHA (22°45′N, 158°W)—located in the eastern portion of the oligotrophic North Pacific Subtropical Gyre (NPSG)—the Hawaii Ocean Time-series (HOT) program routinely measures, at near monthly intervals since October 1988, a suite of physical, biological, and biogeochemical parameters designed to improve our understanding of the processes controlling the oceanic C cycle (Karl and Lukas 1996). This long record has allowed the study of seasonal, inter-annual, and decadal variability in ^{14}C-based primary production (^{14}C-PP) and particulate matter export via sinking particles (Karl et al. 2021). After three decades of observations, the seasonal cycle in ^{14}C-PP is well characterized and contributes about 30% to the total observed variance (Karl et al. 2021). Due to losses of labeled C through respiration, grazing, and excretion of dissolved organic C during the incubations, the ^{14}C-PP rates measured by the HOT program (over sunrise-to-sunset incubations) are less than gross primary C production but probably greater than net primary C production—the balance between gross primary C production and photoautotrophic respiration (Marra 2002; Karl et al. 2021; Marra et al. 2021). Where exactly ^{14}C-PP estimates lie in relation to net and gross C production cannot be easily constrained as it can vary as a function of phytoplankton community structure (Pei and Laws 2013), net growth rate (Halsey et al. 2011, 2013; Pei and Laws 2014), and the production of labeled dissolved organic C by processes such as exudation, grazing, and viral lysis (Karl et al. 1998; Viviani et al. 2015).

Global and regional-scale satellite assessments of primary production are currently validated using observations of ^{14}C-PP (Westberry et al. 2023 and references therein). More recently, the development and refinement of non-incubation approaches to measure gross oxygen production (GOP), including the analysis of the triple isotopic composition of dissolved O_2 (Juranek and Quay 2013 and references therein), as well as the diel cycle of dissolved O_2 (e.g., Ferrón et al. 2015; Nicholson et al. 2015; Barone et al. 2019) and particulate organic C estimated from bio-optical properties (e.g., White et al. 2017; Stoer and Fennel 2022), have increased our ability to characterize oceanic primary production and understand its variability (Huang et al. 2021; Johnson and Bif 2021; Stoer and Fennel 2022). In addition, it is now possible to quantify gross O_2 production with the ^{18}O-water incubation method (^{18}O-labeled gross O_2 production [^{18}O-GOP]) using membrane inlet mass spectrometry (MIMS) (Ferrón et al. 2016; IOCCG 2022), making GOP measurements more accessible and enabling at sea analyses of samples, which in turn can be pivotal for validating non-incubation methods as well as emerging satellite gross primary production models (Westberry et al. 2023).

In this study, we compile a 5-year time series of metabolic rates at or near Station ALOHA to investigate their patterns of variability. Our observations provide an improved understanding of the vertical and seasonal variability in GOP and CR in the oligotrophic ocean and highlight the need to better characterize CR variability.

Materials and methods

Sample collection and incubation

Sampling for this study was conducted between April 2015 and July 2020 on oceanographic cruises at or in the vicinity of Station ALOHA (Supporting Information Table S1; Fig. S1). These cruises included regular HOT cruises and research expeditions from the Simons Collaboration on Ocean Processes and Ecology (SCOPE) program. Whole seawater samples were collected using standard 12-L polyvinyl chloride Niskin®-type bottles equipped with Teflon®-coated springs and Viton® O-rings and attached to a conductivity-temperature-depth rosette sampler. Seawater samples were collected from six depths within the euphotic zone (5, 25, 45, 75, 100, and 125 m), except for the field experiments conducted during 2015, in which the deepest depth (125 m) was not sampled (Supporting Information Table S1).

Seawater for subsequent GOP and CR measurements was sub-sampled into volume-calibrated quartz bottles (~ 150 mL) with flat-bottom ground-glass stoppers. Before each cruise, the bottles and stoppers were rinsed with dilute detergent (Liquinox® or Citranox®, 1% vol/vol) and Milli-Q water (resistivity > 18.2 MΩ·cm at 25°C), soaked in dilute HCl (10% vol/vol) for at least 24 h, and thoroughly rinsed with Milli-Q water. During sampling, the bottles were rinsed with seawater and filled from bottom to top using acid-washed silicone tubing, allowing the water to overflow at least twice the volume of the bottles. From each depth, three samples were collected as time-zero and three were spiked with labeled water and incubated (dawn to dusk, ~ 11–13 h) at their depth of collection on a free-drifting surface tethered array, alongside bottles for ^{14}C-bicarbonate assimilation measurements (Karl et al. 2021). Incubation samples were spiked with ^{18}O-labeled water (97.6% ^{18}O, Medical Isotopes Inc.). Samples collected between 5 and 45 m were spiked with 650 μL of labeled water, whereas samples collected between 75 and 125 m were spiked with 1000 μL (Ferrón et al. 2016). These additions would bring the δ^{18}O of seawater, relative to the Vienna Standard Mean Ocean Water, to ~ 2000‰ and 3100‰, respectively, which was required for the low productivity NPSG. The time-zero samples were fixed with 0.27 M mercuric chloride solution (~ 0.1% of the total sample volume) at the time of deployment of the array to terminate biological activity. Tapered ground glass stoppers were used to reseal the bottles without introducing air bubbles (IOCCG 2022). The stoppers were held

in place with electrical tape. Then the bottles were slowly inverted three times to mix the mercuric chloride, and subsequently stored upside down in the dark with the neck immersed in Milli-Q water to keep the seal wet to restrict air exchange. The same procedure was applied to fix the incubated samples after the recovery of the array. Samples were analyzed by MIMS either onboard the vessel or in the shore laboratory within 1–6 d of collection (Ferrón et al. 2016).

Primary production from ^{14}C-bicarbonate assimilation

The ^{14}C method was also used to estimate primary production (^{14}C-PP) following HOT standard protocols (available at http://hahana.soest.hawaii.edu/hot/protocols/protocols.html; Karl et al. 2021).

Sample analysis by MIMS

The relative abundances of dissolved $^{18}O^{16}O$ and $^{16}O^{16}O$ as well as O_2 to Ar molar concentration ratios were measured in seawater using a MIMS dissolved gas analyzer (Bay Instruments). The instrument and methodology are described in detail by Ferrón et al. (2016). A standard consisting of filtered (0.2 μm) surface seawater of known salinity (collected at Station ALOHA) and equilibrated with ambient air at 23.00°C ($\pm$ 0.01°C) was used to calibrate the MIMS and account for drift in the signals (Kana et al. 1994; Ferrón et al. 2016). During operation, the standard was typically analyzed every three samples (at intervals of $\sim$ 20 min).

The concentrations of dissolved O_2 and Ar in the standard were calculated using the solubility equations of García and Gordon (1992) and Hamme and Emerson (2004), respectively. The isotopic composition of dissolved O_2 in the standard was calculated using the solubility fractionation reported by Kroopnick and Craig (1972).

Determination of metabolic rates

Daily GOP (mmol O_2 m^{-2} d^{-1}) was determined from the change in the isotope ratio of dissolved O_2 over the incubation period, covering one photoperiod (Bender et al. 1987, 1999; Kiddon et al. 1995):

$$\mathrm{GOP} = \left[\frac{^{18}R(\mathrm{O_2})_{\mathrm{final}} - {}^{18}R(\mathrm{O_2})_{\mathrm{initial}}}{^{18}R(\mathrm{H_2O}) - {}^{18}R(\mathrm{O_2})_{\mathrm{initial}}}\right] \times [\mathrm{O_2}]_{\mathrm{initial}} \quad (1)$$

where $^{18}R(O_2)_{initial}$ and $^{18}R(O_2)_{final}$ are the initial and final isotope ratios ($^{18}O/^{16}O$) for dissolved O_2, $[O_2]_{initial}$ is the initial dissolved O_2 concentration, and $^{18}R(H_2O)$ is the isotope ratio of the incubation water, which is calculated based on the amount of labeled water added and the calibrated volume of the incubation flask. On average, the standard deviation (SD hereafter) and coefficient of variation of the triplicate GOP measurements in the top 45 m were 0.12 mmol O_2 m^{-3} d^{-1} and $\sim$ 10%, respectively, whereas in the 75–125 m region they were 0.05 mmol O_2 m^{-3} d^{-1} and $\sim$ 14%, respectively. On average, the SD (and standard error) for GOP measurements was 0.09 (0.05) mmol O_2 m^{-3} d^{-1}.

The net O_2 change (ΔO_2, mmol O_2 m^{-3}) over the incubation period can be simultaneously determined in the same incubation bottle as GOP from the net change in O_2/Ar (Bender et al. 1999):

$$\Delta \mathrm{O_2} = \left[\frac{(\mathrm{O_2/Ar})_{\mathrm{final}}}{(\mathrm{O_2/Ar})_{\mathrm{initial}}} - 1\right] \times [\mathrm{O_2}]_{\mathrm{initial}} \quad (2)$$

where $(O_2/Ar)_{initial}$ and $(O_2/Ar)_{final}$ are the initial and final O_2/Ar ratios. Assuming that photosynthesis and respiration are the only two processes affecting the O_2/Ar molar ratio in the incubation bottle, and that CR is constant throughout the day, then CR (mmol O_2 m^{-3} d^{-1}) can be calculated from GOP and ΔO_2 (Ferrón et al. 2016):

$$\mathrm{CR} = \frac{24}{\Delta t} \times [\mathrm{GOP} - \Delta \mathrm{O_2}] \quad (3)$$

where Δt is the time period between the poisoning of time-zero and incubated samples (h). Note that estimates of CR were determined from triplicate incubation bottles. Triplicate measurements of CR showed substantially higher variability than GOP, particularly between February 2017 and April 2018 (Supporting Information Fig. S2). During this time, occasional extreme values in CR were observed (Supporting Information Fig. S3). We identified outliers as values exceeding or falling below specific thresholds. The upper threshold was calculated as the third quartile plus twice the interquartile range, and the lower threshold was calculated as the first quartile minus twice the interquartile range. While this method did not identify any outliers in GOP, 19 out of 694 CR measurements (< 3%) were categorized as outliers and subsequently removed from further analysis (Supporting Information Fig. S3). This removal, targeted at individual replicates, resulted in a $\sim$ 1% reduction of mean CR values. Removed CR outliers were distributed throughout the water column but were more abundant at or below 100 m ($\sim$ 63%) and did not exhibit a distinct seasonal pattern. Even after outlier removal, the period between February 2017 and April 2018 continued to display higher variability in CR replicates compared to the rest of the time series (Supporting Information Fig. S2). On average, the SD (and standard error) of triplicate CR measurements during this period was 0.32 (0.18) mmol O_2 m^{-3} d^{-1}, while outside of this period it was 0.21 (0.12) mmol O_2 m^{-3} d^{-1}, with the overall values for the entire time series being 0.26 (0.15) mmol O_2 m^{-3} d^{-1}. On average, the coefficient of variation was approximately 22% in the top 45 m and 36% in the 75–125 m layer. In fewer than 6% of cases (14 out of 236), derived CR values were negative. While negative values are distributed throughout the year, they were predominantly located in the lower euphotic zone (75–125 m), with 79% of cases occurring at 125 m. Although these negative CR values lack biological

meaning, as they would imply that ΔO_2 is larger than gross production, we chose not to exclude negative CR values under the premise that the different sources of uncertainty would equally bias CR estimates high and low, and excluding all negative values would only remove estimates biased low, as reasoned by Barone et al. (2019).

Light–dark O_2 method

We compare our rate measurements with a compilation of GOP and CR measured during HOT cruises at Station ALOHA by the light–dark O_2 method, as described in detail by Williams et al. (2004). The compilation includes data collected from May 2001 to May 2002 (reported by Williams et al. 2004) as well as previously unpublished data collected from June 2005 to June 2007, using the same methodology. From nighttime CTD casts, 24 discrete samples (8 replicates each for time-zero, light, and dark bottles) were collected into volume-calibrated borosilicate ground glass stoppered bottles ($\sim$ 125 mL). The light and dark bottles were deployed in a free-drifting array before sunrise and incubated in situ for approximately 24 h. Time-zero samples were fixed for Winkler titration immediately after the array was deployed, and light and dark bottles immediately after the array was recovered. The depths sampled for Winkler measurements were 5, 25, 45, 75, 100, and 150 m for the earlier data (2001–2002); and 5, 25, 45, 75, 100, and 125 m for the later data (2006–2007). The change in O_2 relative to time-zero samples in the light and dark bottles provides a measurement of net community production (NCP) and CR, respectively. Gross oxygen production is derived as the sum of NCP and CR. The mean standard errors for NCP, GOP, and CR in the compiled dataset were 0.09, 0.09, and 0.08 mmol O_2 m^{-3} d^{-1}, respectively.

Data analysis

Areal rates of ^{18}O-GOP, ^{14}C-PP, and CR (mmol m^{-2} d^{-1}) were calculated using trapezoidal depth integration, and their uncertainties were determined by propagating the SD of triplicate measurements at each depth (Karl et al. 2021). As the shallowest sample is collected at 5 m, integration to the surface is done by assuming the rates in the upper 5 m layer to be homogeneous. In a total of 5 vertical profiles of ^{18}O-GOP and CR conducted during 2015, rates were not measured at 125 m (Supporting Information Table S1). In those cases, the 0–125 m depth-integrated rates were estimated from the 0–100 m depth-integrated values using a linear regression (model II fit) between 0–125 and 0–100 m integrated rates obtained from the rest of the dataset. The correlation equations used to transform 0–100 to 0–125 m depth-integrated ^{18}O-GOP and CR are, respectively: $Y = -1.294\ (\pm 1.340) + 1.083\ (\pm 0.018)X$, $r^2 = 0.991$, $p < 0.00001$; $Y = -1.753\ (\pm 3.391) + 1.144\ (\pm 0.043)X$, $r^2 = 0.960$, $p < 0.00001$.

Meteorological definitions of seasons were used, with winter covering December to February, spring March to May, summer June to August, and fall September to November.

Unless otherwise specified, comparisons between two groups of data were done using the Wilcoxon rank-sum test at a significance level of $p < 0.05$.

When model II linear regressions were applied, they were determined using the geometric mean or reduced major axis method.

Results

Vertical variability in primary production and respiration

Vertical profiles of ^{18}O-GOP, ^{14}C-PP, and CR showed the expected decrease in rates with depth throughout the

Table 1. Summary of ^{18}O-GOP, CR, and ^{14}C-PP for each depth, including the range and mean ± SD. The ratios of mean ^{18}O-GOP to ^{14}C-PP (^{18}O/^{14}C), and the ratios of mean ^{18}O-GOP to CR (± propagated SD) are also provided.

m	mmol O_2 m^{-3} d^{-1}		mmol C m^{-3} d^{-1}	mol O_2 (mol C)$^{-1}$	mol O_2 (mol O_2)$^{-1}$
Depth	^{18}O-GOP	CR	^{14}C-PP	^{18}O/^{14}C	^{18}O-GOP/CR
5	0.53 to 2.32	0.10 to 2.05	0.28 to 0.92	1.0 to 2.7	0.5 to 10.6
	0.98 ± 0.31	0.84 ± 0.46	0.56 ± 0.15	1.7 ± 0.4*	1.2 ± 0.5*
25	0.53 to 2.26	0.16 to 2.12	0.21 to 0.95	1.3 to 3.1	0.5 to 6.0
	1.07 ± 0.32	0.97 ± 0.49	0.57 ± 0.14	1.9 ± 0.3*	1.1 ± 0.5*
45	0.28 to 1.45	−0.14 to 2.16	0.13 to 0.90	1.2 to 3.5	−5.8 to 5.0
	0.86 ± 0.22	0.82 ± 0.46	0.49 ± 0.13	1.8 ± 0.3*	1.1 ± 0.5*
75	0.17 to 0.83	−0.39 to 1.73	0.11 to 0.52	0.7 to 2.6	−0.8 to 3.5
	0.52 ± 0.17	0.78 ± 0.49	0.30 ± 0.10	1.8 ± 0.4*	0.7 ± 0.4*
100	0.10 to 0.61	0.03 to 1.75	0.06 to 0.42	0.6 to 3.3	0.1 to 8.5
	0.28 ± 0.13	0.55 ± 0.42	0.18 ± 0.09	1.5 ± 0.5*	0.5 ± 0.4*
125	−0.02 to 0.24	−0.43 to 0.94	0.02 to 0.17	−0.4 to 3.2	−11.2 to 9.1
	0.11 ± 0.07	0.22 ± 0.34	0.07 ± 0.04	1.5 ± 0.6*	0.5 ± 0.7*

^{14}C-PP, ^{14}C-based primary production; CR, community respiration; ^{18}O-GOP, ^{18}O-labeled gross oxygen production.
*Ratio of the mean values ± propagated SD.

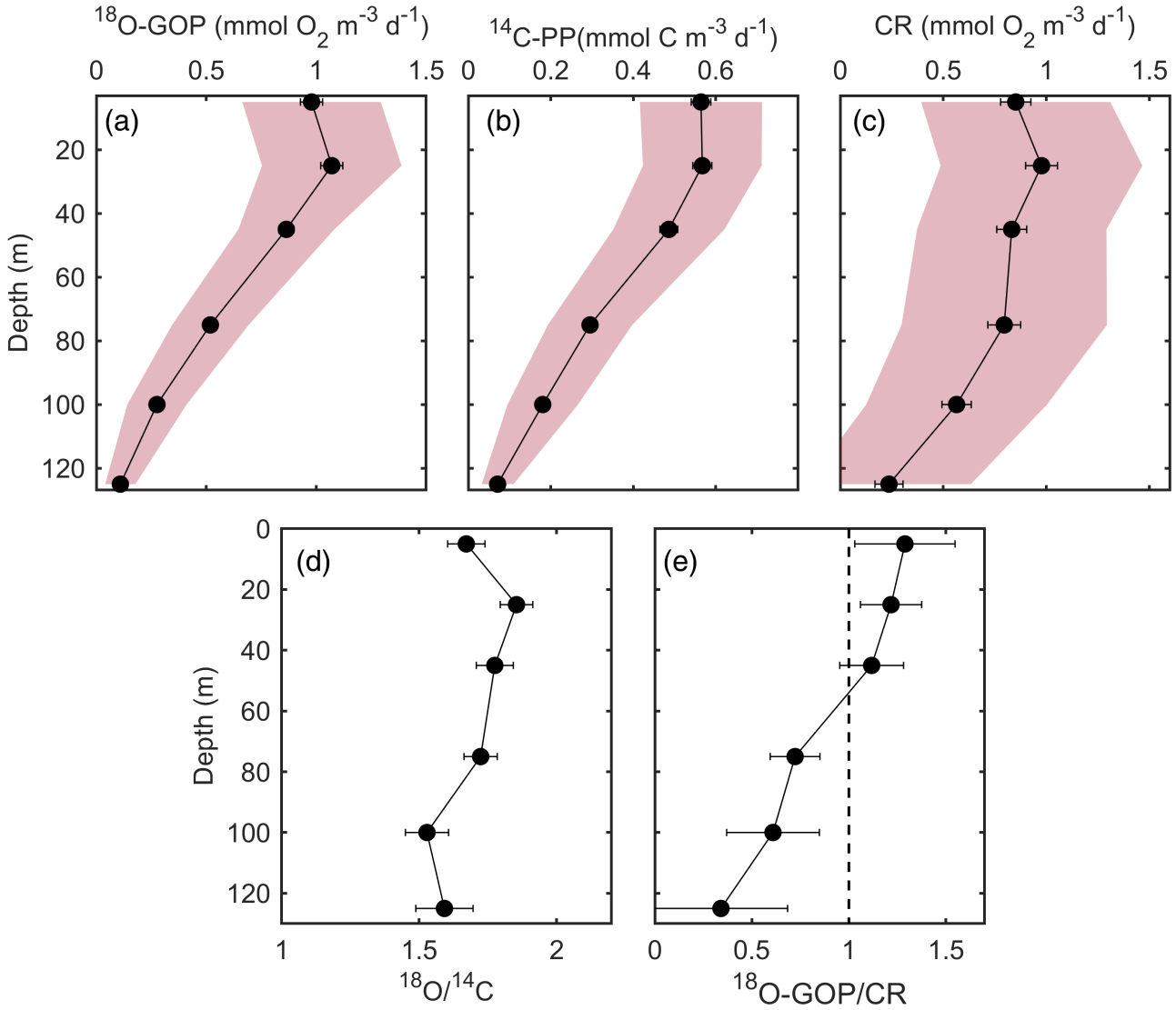

Fig. 1. Mean depth profiles of (**a**) ^{18}O-GOP, (**b**) ^{14}C-PP, and (**c**) CR. Error bars in (**a**–**c**) represent the standard error, while the shaded red areas represent ± 1 SD of the mean values. (**d**) Ratio of mean ^{18}O-GOP to mean ^{14}C-PP for each depth (± propagated standard error) in mol O_2 (mol C)$^{-1}$. (**e**) Ratio of mean ^{18}O-GOP to mean CR for each depth (± propagated standard error). The vertical dashed line in (**e**) represents a ratio of 1, where the system would be in metabolic balance (GOP = CR). ^{14}C-PP, ^{14}C-based primary production; CR, community respiration; ^{18}O-GOP, ^{18}O-labeled gross oxygen production.

euphotic zone (Table 1; Fig. 1). The depth distributions and the variability of ^{18}O-GOP and ^{14}C-PP were very similar, with ^{18}O-GOP consistently exceeding ^{14}C-PP at all depths ($p < 0.03$). Community respiration exhibited substantially more variability within each depth compared to both ^{18}O-GOP and ^{14}C-PP, as well as previous dark CR measured by the light–dark O_2 method (Supporting Information Fig. S4). In addition, the decline of CR with depth was less pronounced than for primary production (Table 1; Fig. 1). For example, mean ^{18}O-GOP and ^{14}C-PP at 125 m represented ~ 10–12% of the mean values at 25 m, whereas mean CR at 125 m was ~ 23% of the value at 25 m. In the top 45 m of the euphotic zone, ^{18}O-GOP exceeded CR ($p = 0.001$), indicating autotrophy (Table 1; Fig. 1e). In the lower portion of the euphotic zone (75–125 m) CR surpassed ^{18}O-GOP ($p < 0.0001$), indicating heterotrophy, and the ratio of mean ^{18}O-GOP to CR fell below 1 (Table 1; Fig. 1e).

The ratios of mean ^{18}O-GOP to mean ^{14}C-PP (mol O_2 (mol C)$^{-1}$) were relatively constant with depth, ranging from 1.9 ± 0.3 mol O_2 (mol C)$^{-1}$ (± propagated SD) at 25 m to 1.5 ± 0.6 mol O_2 (mol C)$^{-1}$ at 125 m (Table 1; Fig. 1). There was a significant positive correlation between rates of ^{18}O-GOP and ^{14}C-PP ($r^2 = 0.86$, $p < 0.0001$; Supporting Information Fig. S9), indicating that both measures of productivity tracked each other well. The slope of a model II

regression fit of ^{18}O-GOP against ^{14}C-PP was 1.88 ± 0.05 (n = 222). Rates of ^{18}O-GOP were also significantly correlated with ΔO_2 (r^2 = 0.39, p < 0.0001) and CR (r^2 = 0.33, p < 0.0001).

Depth-integrated rates

Depth-integrated (0–125 m) values of ^{18}O-GOP and ^{14}C-PP varied fourfold (Table 2; Fig. 2), averaging 80 ± 19 (± SD) mmol O_2 m^{-2} d^{-1} and 45 ± 10 (± SD) mmol C m^{-2} d^{-1}, respectively. Because not all the seasons were equally represented in our time series (Supporting Information Fig. S1), we calculated the seasonally unbiased annual fluxes by averaging the mean values from each season (Table 2, last row). Mean annual ^{18}O-GOP and ^{14}C-PP were 74 ± 14 mmol O_2 m^{-2} d^{-1} and 43 ± 5 mmol C m^{-2} d^{-1}, respectively. Depth-integrated values of ^{18}O-GOP and ^{14}C-PP were positively correlated (r^2 = 0.57, GOP = −7.9 (± 10.8) + 1.9 (± 0.2) ^{14}C-PP, p < 0.0001).

Depth-integrated (0–125 m) CR varied fivefold, averaging 89 ± 37 mmol O_2 m^{-2} d^{-1}. The observed variability in CR was higher than previous measurements using the light–dark Winkler method (Supporting Information Fig. S5). The seasonally unbiased annual mean (± SD) for this study was 80 ± 18 mmol O_2 m^{-2} d^{-1} (Table 2; Fig. 2). Depth-integrated rates of CR were significantly but weakly correlated with ^{18}O-GOP (r^2 = 0.27, p = 0.001), but not with ^{14}C-PP (p = 0.11), and they were not significantly different from ^{18}O-GOP (p = 0.52).

On average, > 55% of 0–125 m depth-integrated ^{18}O-GOP and ^{14}C-PP took place in the top 45 m of the water column. In contrast, vertical changes in CR were less pronounced, with 45% of depth-integrated CR occurring in the upper 45 m (Fig. 3). There was an offset of approximately 10 m in the depth where cumulative CR reached 50% of its 0–125 m integrated value (51 m), compared to ^{18}O-GOP and ^{14}C-PP (40–41 m, Fig. 3).

Temporal variability in primary production and respiration

Over the 5-yr study period, primary production exhibited an occasional extreme value compared to the 30-yr HOT observations (Supporting Information Fig. S6), with the minimum in ^{14}C-PP for the entire dataset (post-January 1989) occurring in February 2018 and relatively elevated production in August 2017 (Fig. 2; Supporting Information Fig. S6; Karl et al. 2021). The minimum in February 2018 coincided with a cloudy day that resulted in a very low daily integrated surface photosynthetically available radiation (7.7 mol quanta m^{-2} d^{-1}) compared to light flux measured on both the previous and subsequent days (35.0 and 19.6 mol quanta m^{-2} d^{-1}, respectively). The ^{18}O-GOP and the ^{14}C-PP varied by

Table 2. Summary of depth-integrated fluxes. Each row provides either the range or the mean ± SD of depth-integrated (0–125 m) ^{18}O-GOP, CR, ^{14}C-PP, ^{18}O-GOP to ^{14}C-PP ratios, and ^{18}O-GOP to CR ratios for all data during the study period as well as for each season. Values in parentheses represent median values. Annual values are determined as the mean (± SD) of the four seasons, to avoid bias toward summer months. The mean temperature (± SD) in the upper 125 m at Station ALOHA for each season during the period 2015–2020 is also provided.

^{18}O-GOP	CR	^{14}C-PP	^{18}O/^{14}C	^{18}O-GOP/CR
mmol O_2 m^{-2} d^{-1}		mmol C m^{-2} d^{-1}	mol O_2 (mol C)$^{-1}$	mol O_2 (mol O_2)$^{-1}$
All data				
35–134	37–187	18–75	1.2–2.5	0.4–2.0
80 (77) ± 19	89 (83) ± 37	45 (46) ± 10	1.8 ± 0.3*	0.9 ± 0.3*
Winter (December–February), T = 24.1 ± 0.8°C				
35–80	37–152	18–50	1.2–2.0	0.4–2.0
61 (65) ± 14	70 (53) ± 44	40 (43) ± 10	1.5 ± 0.2*	0.9 ± 0.6*
Spring (March–May), T = 23.9 ± 0.5°C				
58–83	46–114	30–52	1.5–2.4	0.7–1.5
71 (70) ± 8	79 (88) ± 25	38 (37) ± 7	1.8 ± 0.3*	0.9 ± 0.2*
Summer (June–August), T = 25.0 ± 0.4°C				
74–134	60–187	42–75	1.4–2.5	0.5–1.7
93 (87) ± 17	104 (108) ± 37	52 (49) ± 8	1.8 ± 0.3*	0.9 ± 0.3*
Fall (September–November), T = 25.2 ± 0.6°C				
60–85	43–85	33–50	1.6–2.0	0.8–1.4
73 (73) ± 10	66 (68) ± 17	42 (42) ± 6	1.7 ± 0.2*	1.1 ± 0.3*
Annual unbiased mean				
74 ± 14	80 ± 18	43 ± 5	1.7 ± 0.1*	0.9 ± 0.3*

^{14}C-PP, ^{14}C-based primary production; CR, community respiration; ^{18}O-GOP, ^{18}O-labeled gross oxygen production.
*Ratio of the mean values ± propagated SD.

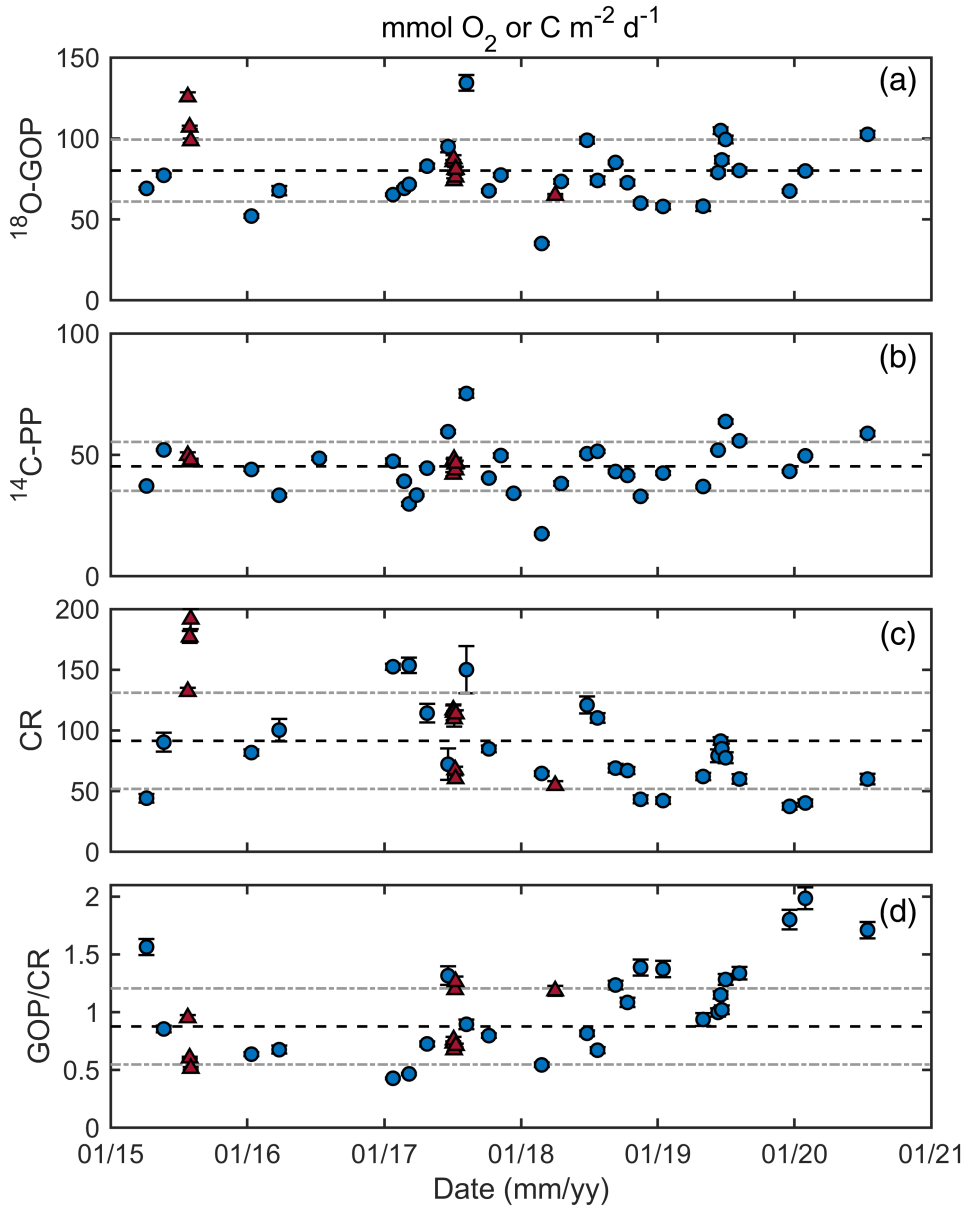

Fig. 2. Time series of daily 0–125 m depth-integrated rates of (**a**) ^{18}O-GOP, (**b**) ^{14}C-PP, (**c**) CR, and (**d**) the ^{18}O-GOP to CR ratios. Blue circles and red triangles are from field experiments conducted at or in the vicinity of Station ALOHA (Supporting Information Table S1), respectively. Error bars are the propagated SD as in Karl et al. (2021). The horizontal dash black lines represent the mean values for the time series (Table 2), with ± 1 SD shown as horizontal gray dot-dash lines. ^{14}C-PP, ^{14}C-based primary production; CR, community respiration; ^{18}O-GOP, ^{18}O-labeled gross oxygen production.

~ 22–24% during our study period (coefficient of variation), similar to the variation (~ 25%) observed in the full 30-yr time series of ^{14}C-PP. In contrast, 0–125 m depth-integrated CR demonstrated greater variability (~ 42%) (Fig. 2c) and appeared to decrease over the period of this study (slope = −0.039 ± 0.010 (mmol O_2 m^{-2} d^{-1}) d^{-1}, $r^2 = 0.30$, $p = 0.0005$). The downward trend was partly driven by the high CR values measured in July–August 2015, where measurements were conducted during a SCOPE cruise targeting an anticyclonic eddy to the northeast of Station ALOHA (Wilson et al. 2017; Supporting Information Table S1). Exclusion of measurements made outside of Station ALOHA (red triangles in Fig. 2) results in no significant decrease in CR ($p = 0.07$). Neither ^{18}O-GOP nor ^{14}C-PP displayed a significant trend during the study period. The ^{18}O-GOP to CR ratios showed considerable variability, with particularly high values (> 1.7) on three occasions when CR was particularly low.

Depth-integrated ^{18}O-GOP varied seasonally (Fig. 4a), with values greatest in the summer (June–August) and lowest in the winter (December–February; $p < 0.0001$, one-way

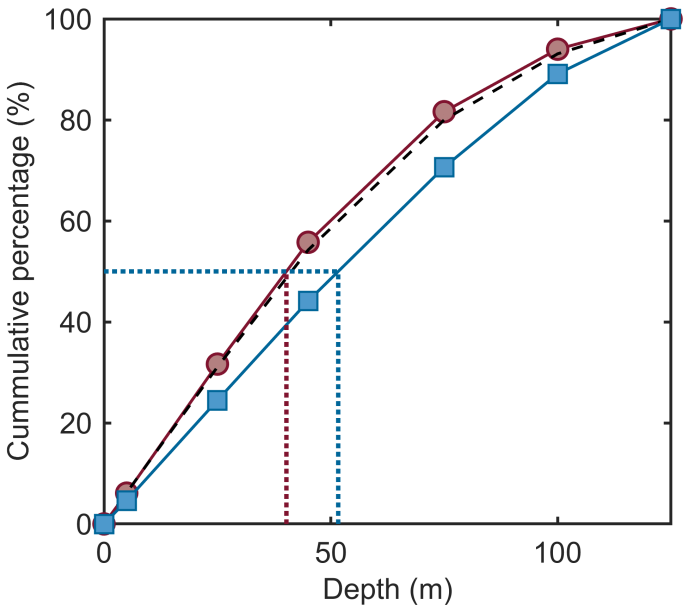

Fig. 3. Cumulative percentage of depth-integrated ^{18}O-GOP (red circles), ^{14}C-PP (dashed black line), and CR (blue squares). Dotted red and blue vertical lines represent the depths at which the percentage of depth-integrated ^{18}O-GOP and CR is 50% of the total for the 0–125 m integral (40 and 50 m, respectively). ^{14}C-PP, ^{14}C-based primary production; CR, community respiration; ^{18}O-GOP, ^{18}O-labeled gross oxygen production.

ANOVA). Similarly, ^{14}C-PP was greatest in summer and lower in spring (March–May) and winter ($p = 0.0005$, one-way ANOVA) (Fig. 4d). Seasonality in 0–125 m depth-integrated productivity was more pronounced for ^{18}O-GOP than for ^{14}C-PP, with mean values in summer exceeding those in winter by 53% and 31%, respectively. Seasonality in primary production was also more pronounced in the lower euphotic zone (75–125 m, Fig. 4c,f) compared to the well-lit portion of the upper ocean (0–45 m, Fig. 4b,e). Mean summertime depth-integrated (0–45 m) ^{18}O-GOP and ^{14}C-PP values were 41% and 24% larger than mean winter values, respectively. In difcontrast, mean summer values in the lower euphotic zone (75–125 m) were 95% and 44% larger than winter values, respectively. Ratios of mean depth-integrated (0–125 m) ^{18}O-GOP to ^{14}C-PP (^{18}O/^{14}C) for each season ranged between 1.5 ± 0.3 mol O_2 (mol C)$^{-1}$ in winter and 1.8 ± 0.3 mol O_2 (mol C)$^{-1}$ in spring and summer (Table 2). In the lower euphotic zone (75–125 m), ^{18}O/^{14}C averaged 1.3 ± 0.3 mol O_2 (mol C)$^{-1}$ in winter, significantly lower than for all the other seasons ($p = 0.0001$, one-way ANOVA).

The rates of depth-integrated (0–125 m) CR exhibited similar seasonal patterns to those of primary production (Fig. 4g), with mean values in summer exceeding those in winter by 49%, but the variations were not statistically significant ($p = 0.128$, one-way ANOVA). This is probably due to the higher variability associated with CR measurements. If the winter outlier (Fig. 4g) is excluded from the statistical test, the seasonality becomes statistically significant ($p = 0.024$, one-way ANOVA). The ratios of ^{18}O-GOP to CR integrated over the top 125 m did not vary significantly with the seasons ($p = 0.715$).

Discussion

Comparison with the light–dark O_2 method

The mean depth-integrated (0–125 m) GOP derived from the compilation of light–dark O_2 measurements (O_2-GOP) conducted during 2001–2002 and 2005–2007 was 55 ± 15 mmol O_2 m^{-2} d^{-1}, 32% lower than the annual ^{18}O-GOP derived from this study (Table 2). The difference between these two datasets was significant for all depths ($p < 0.035$; Fig. 5a; Supporting Information Table S3), while mean rates of ^{14}C-PP did not differ at any depth between the two study periods ($p > 0.05$; Fig. 5b; Supporting Information Table S2). Previous studies measured ^{18}O-GOP at Station ALOHA to depths of 100 m (Juranek and Quay 2005; Quay et al. 2010), and the rates of ^{18}O-GOP (0–100 m) reported here are not significantly different from those reported by Quay et al. (2010) ($p > 0.05$), with annual means from both studies nearly identical: 70 ± 12 and 71 ± 16 mmol O_2 m^{-2} d^{-1}, respectively. The ^{18}O-GOP differs from O_2-GOP in that the former is a measure of the total O_2 evolution from the splitting of water in photosystem II, including the fraction that is not involved in C fixation, for example, when O_2 gets subsequently photo-reduced back to water through the so-called water–water cycles or is lost to photorespiration (Bender et al. 1987, 1999). Results based on experiments using the chlorophyte *Dunaliella tertiolecta* and the marine diatom *Thalassiosira weissflogii* indicate that these pathways can contribute up to 25% of the ^{18}O-GOP (Halsey et al. 2010, 2013). Consistent with our findings, pairwise comparisons of ^{18}O-GOP and O_2-GOP have found that the isotopic method often yields greater rates, with a median ^{18}O-GOP to O_2-GOP ratio of 1.3 (Regaudie-de-Gioux et al. 2014).

If we interpret the difference in mean GOP between this study and the light–dark O_2 method at Station ALOHA as the fraction of the photosynthetic electron flow directed to water–water cycles and photorespiration, we would expect our CR estimates to exceed those derived from the light–dark O_2 method by an even a larger extent. In contrast, the mean annual 0–125 m depth-integrated CR for this study, 80 ± 18 mmol O_2 m^{-2} d^{-1}, is very similar to that derived from the compilation of Winkler measurements, 77 ± 16 mmol O_2 m^{-2} d^{-1} ($p = 0.276$). Hence, the difference in GOP between these studies does not appear to be explained solely due to the reduction of O_2 by water–water cycles and photorespiration; such a difference could reflect changes in these ecosystem processes between the two time periods (separated by a decade), or stem from methodological differences. For example, the light–dark O_2 method, as

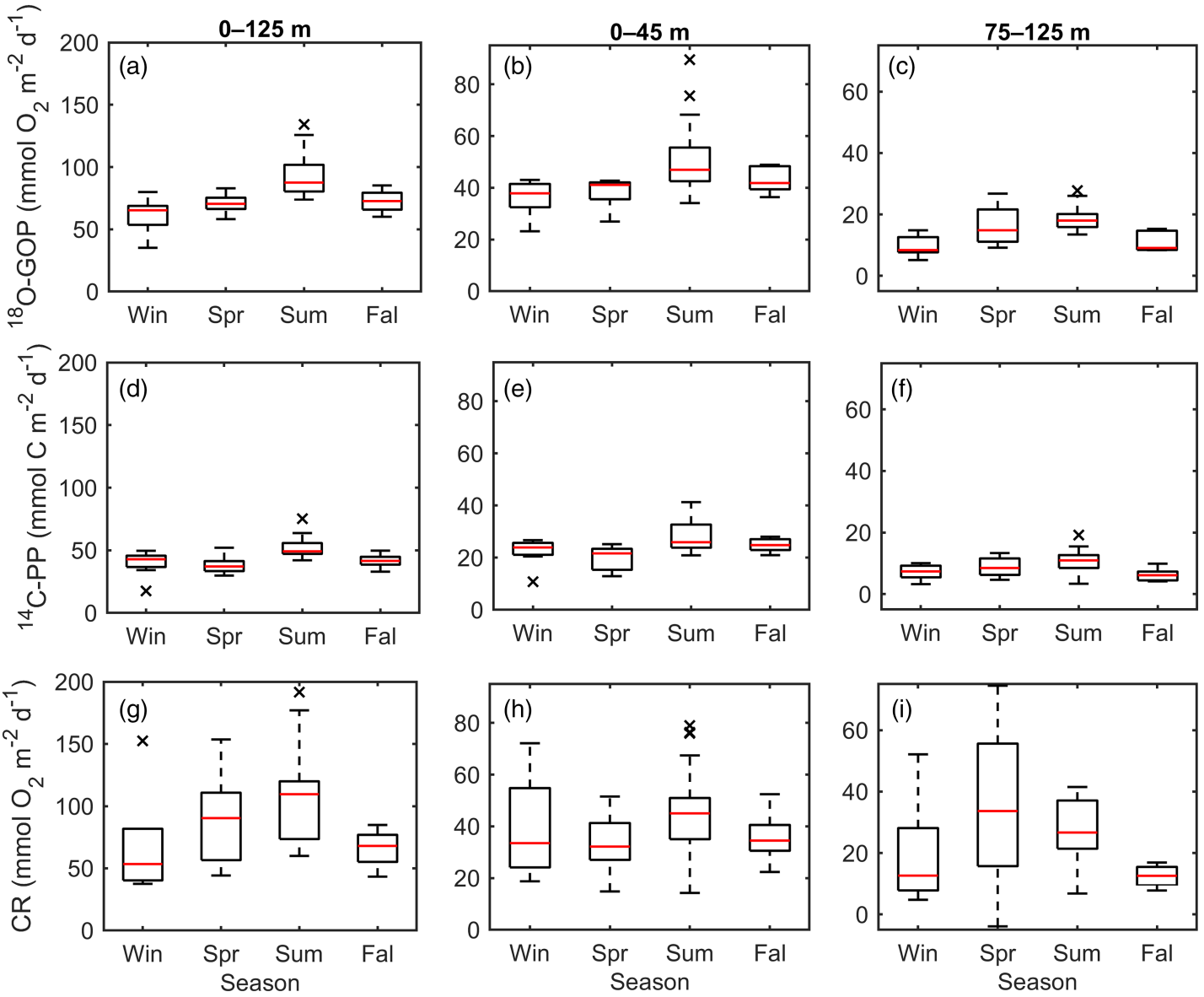

Fig. 4. Plots of seasonal variability in metabolic rates. Box and whisker plot of depth-integrated ^{18}O-GOP (**a**–**c**), ^{14}C-PP (**d**–**f**), and CR (**g**–**i**) for each season. Left panels show depth-integrated values for the entire euphotic zone (0–125 m), while middle and right panels show the upper (0–45 m) and lower (75–125 m) portions of the euphotic zone. The red lines represent the median, and the bottom and top edges of the boxes indicate the 25th and 75th percentiles, respectively. The whiskers extend to the most extreme data points, excluding outliers (black crosses), defined here as 1.5 times the interquartile range. ^{14}C-PP, ^{14}C-based primary production; CR, community respiration; ^{18}O-GOP, ^{18}O-labeled gross oxygen production; Win, winter; Spr, spring; Sum, summer; Fal, fall.

employed at Station ALOHA, measures CR over a 24-h period (sunrise to sunrise) in the dark, and assumes that CR is the same under light and dark conditions and is decoupled from contemporaneous primary production (note that the incubations started at sunrise, after natural communities spent the 10–12 h in the dark). In contrast, we estimate CR during daytime hours under in situ light conditions, derived as the difference between ^{18}O-GOP and the net O_2 change; daily CR was calculated by extrapolating this daytime rate to 24 h, assuming constant CR. Any substantial daily segregation in light-dependent or dark respiration rates, as has been reported for some diazotrophs (Kana 1992; Stöckel et al. 2008), could potentially bias our estimates. Given these differences, the similarity between both CR datasets is surprising, as it would in principle indicate that CR is independent of contemporaneous primary production, that CR is constant throughout the day, and that the losses of O_2 to water–water cycles and photorespiration are minimal (contrary to what the comparison of ^{18}O-GOP and light–dark GOP indicates).

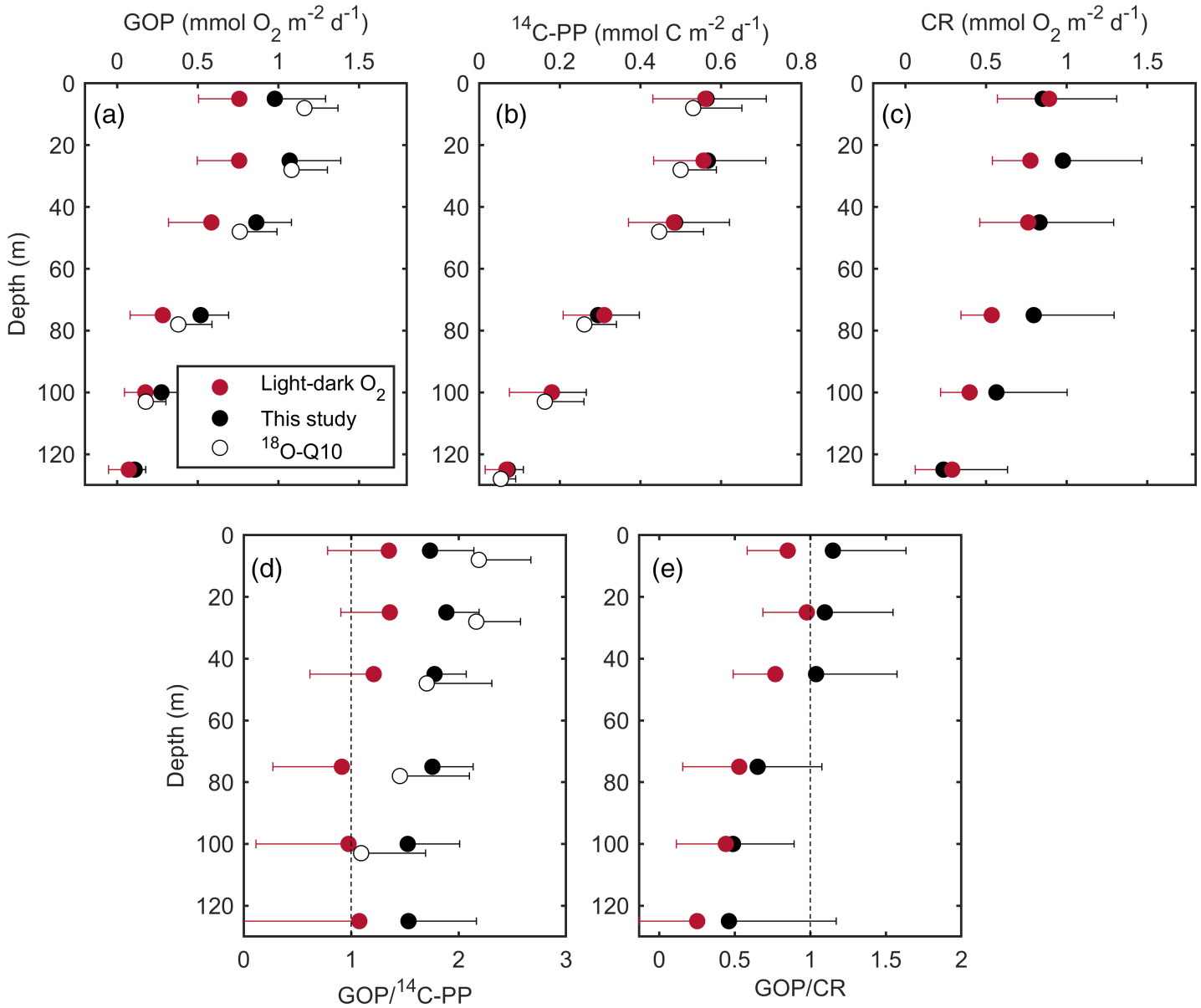

Fig. 5. Comparisons between the mean vertical profiles (± SD) of (**a**) GOP, (**b**) ^{14}C-PP, (**c**) CR, (**d**) the ratio of mean GOP to mean ^{14}C-PP (mol O_2 (mol C) $^{-1}$) (+ or − propagated SD), and (**e**) the ratio of mean GOP to mean CR (+ or − propagated SD), from the time-series observations presented in this study (black circles), data collected in the past at Station ALOHA using the light–dark O_2 method during 2001–2002 (Williams et al. 2004) and 2005–2007 (red circles), as well as by Quay et al. (2010) using the ^{18}O-water incubation method during 2006–2008 (white circles). The markers for the latter have been offset 3 m below the collection depth for easier visualization. ^{14}C-PP, ^{14}C-based primary production; CR, community respiration; ^{18}O-GOP, ^{18}O-labeled gross oxygen production.

Seasonal variability in metabolic rates

Our 5-yr observation period at Station ALOHA was characterized by unusually warm, low-salinity, and low-density surface ocean waters compared to the > 30-yr HOT record (Karl et al. 2021; Supporting Information Fig. S7). During this time, both measures of primary production, ^{18}O-GOP and ^{14}C-PP, showed significant seasonality. During the summer, rates of ^{18}O-GOP were 1.5 times higher than in winter (Fig. 4; Table 2). Such seasonality is consistent with Quay et al. (2010), where the mean summer to winter ratio was 1.5 (Supporting Information Fig. S8). In contrast, ^{14}C-PP and O_2-GOP demonstrated less seasonality, with mean summer to winter ratios of 1.3 (Fig. 4; Supporting Information Fig. S8; Table 2). A potential explanation for greater seasonality in ^{18}O-GOP may reflect seasonal variability in the fraction of newly produced O_2 that gets lost to water–water cycles and photorespiration (and hence is not routed to C fixation). Rates of CR showed a similar seasonal trend than ^{18}O-GOP, with a

mean summer to winter ratio of 1.5, pointing to a seasonal coupling between ^{18}O-GOP and daytime CR, but the seasonal differences were not significant.

While rates of primary production were consistently higher in the top 45 m of the water column, seasonal variations were more pronounced in the lower portion of the euphotic zone (75–125 m) (Fig. 4; Table 2). For ^{18}O-GOP, values in the lower portion of the euphotic zone were higher in spring and summer compared to winter and fall, with mean rates two times greater in summer than in winter. Seasonality in primary production in the lower euphotic zone is a manifestation of seasonal variations in daily integrated solar irradiance at those depths. For example, the depth of a constant daily integrated photon flux of 0.415 mol quanta m^{-2} d^{-1} (representing the annual average at the 1% light level), varies seasonally by approximately 30 m—from ~ 90 m in the winter to ~ 120 m in the summer. Such changes are due to variations in surface solar intensity, photoperiod, and variations in water column light attenuation (Letelier et al. 2004, 2017). In surface waters, light saturation and seasonal changes in the chlorophyll content of phytoplankton combine to decouple solar irradiance from the seasonal patterns in primary production (Karl et al. 2021).

Variations in the ^{18}O-GOP to ^{14}C-PP ratio

Rates of ^{14}C assimilation, measured in situ using dawn to dusk incubations, have been routinely measured at Station ALOHA since 1988 (Karl et al. 2021). However, only a few studies have measured both ^{18}O-GOP and ^{14}C-PP at this site (Juranek and Quay 2005; Quay et al. 2010; Ferrón et al. 2016). From these studies, only Quay et al. (2010) have the temporal coverage to resolve seasonality (Fig. 5; Supporting Information Fig. S8). In the present study, ^{18}O-GOP and ^{14}C-PP were significantly correlated (Supporting Information Fig. S9), with the slope of a model II regression, including all individual volumetric rates, being 1.88 ± 0.05 (mol O_2 (mol C)$^{-1}$) and the coefficient of determination 0.86 ($n = 222$). In comparison, for the Quay et al. (2010) dataset, this slope is 2.49 ± 0.15 and the coefficient of determination is 0.69 ($n = 95$) (Supporting Information Fig. S9). Combining both datasets, the resulting slope is 2.02 ± 0.05 and the coefficient of determination is 0.81 ($n = 317$), implying ^{18}O-GOP is approximately twice as large as ^{14}C-PP at Station ALOHA. Such findings are in agreement with the average ^{18}O-GOP to ^{14}C-PP (12-h incubation) ratio of ~ 2.0 derived from the Joint Global Ocean Flux Study global compilation, collected across different ocean basins (Laws et al. 2000; Marra 2002; Hendricks et al. 2004; Juranek and Quay 2005). Similarly, the slope of GOP measured by the light–dark O_2 method vs. ^{14}C-PP at Station ALOHA is 1.65 ± 0.10 ($r^2 = 0.50$, $n = 170$), comparable to the slope of 1.83 obtained along a latitudinal transect along the Atlantic Ocean (Serret et al. 2023).

The ratio of the annual mean in 0–125 m depth-integrated ^{18}O-GOP to mean ^{14}C-PP was 1.7 ± 0.1 for this study, similar to 1.8 ± 0.4 derived from the 0 to 100 m depth-integrated values reported by Quay et al. (2010). In comparison, the ratio of GOP from the light–dark O_2 method was 1.2 ± 0.4. Previous studies have shown that the ratio of GOP to ^{14}C-PP at Station ALOHA varies both with season and depth (Williams et al. 2004; Juranek and Quay 2005; Quay et al. 2010). The ^{18}O-GOP to ^{14}C-PP ratio from volumetric rates varied seasonally, with the highest values in spring and the lowest in winter ($p = 0.0002$, one-way ANOVA). The depth-integrated (0–125 m) ^{18}O-GOP to ^{14}C-PP ratios tended to be elevated in spring and lower in winter (Table 2), and this was particularly pronounced in the lower portion of the euphotic zone (75–125 m, $p < 0.0001$, one-way ANOVA), with larger ratios in spring compared to all other seasons. Deepening of isolumes in the spring causes an increase in new primary production in the lower euphotic zone and the consumption of nitrate that has accumulated over the winter (Letelier et al. 2004); such changes could underlie increases in ^{18}O-GOP to ^{14}C-PP ratios.

Prior studies at Station ALOHA found that ^{18}O/^{14}C converged at depth (e.g., Juranek and Quay 2005; Quay et al. 2010; Fig. 5). Quay et al. (2010) reported mean values in ^{18}O/^{14}C ranging from 2.4 at 5 m to 1.1 at 100 m (Fig. 5c), while Williams et al. (2004) found that O_2-GOP/^{14}C were 1.2–1.4 in the upper 50 m, and closer to 1 in the lower euphotic zone (75–150 m). Processes influencing this vertical variation in ^{18}O/^{14}C are not well understood, but may stem from differential rates of labeled dissolved organic C production (Karl et al. 1998), changes in community composition (Pei and Laws 2013), growth/grazing rates (Halsey et al. 2011, 2013; Pei and Laws 2014), and/or the photosynthetic quotient. Whatever the reason behind the previously described vertical patterns in ^{18}O/^{14}C, it is enigmatic that ^{18}O-GOP and ^{14}C-PP in this study did not converge at depth. Our results only show a modest decrease in ^{18}O/^{14}C with depth relative to previous studies—from 1.9 ± 0.3 at 25 m to 1.6 ± 0.4 at 100 m—indicating that even in the lower euphotic zone, ^{18}O-GOP was > 50% larger than ^{14}C assimilation (Table 2; Fig. 5c). It is possible that our findings point to temporal increases in the ^{18}O/^{14}C ratio in the lower euphotic zone. The ^{18}O-GOP in the 75–100 m depth range was significantly higher in this study compared to the earlier data reported by Quay et al. (2010) ($p < 0.0001$). Moreover, Karl et al. (2021) recently reported a sustained long-term increase in ^{14}C-PP in the NPSG between 1989 and 2018 (> 0.7% yr^{-1}), a trend that appears largely driven by changes in the lower euphotic zone (75–125 m). Notably, this upward trend did not coincide with greater export fluxes, but was accompanied by significant increases in particulate C and N, and chlorophyll *a* in the lower euphotic zone (Karl et al. 2021). Additionally, the authors "found no evidence for a systematic change in surface PAR, or photon fluxes" in the lower euphotic zone, and attributed these trends to an increase in the horizontal supply of nutrients from enhanced anthropogenic atmospheric deposition to the northwest of Station

ALOHA, through subducted North Pacific Tropical Water. Although our observations do not reveal significant temporal trends in either ^{18}O-GOP or ^{14}C-PP, such long-term trends are difficult to detect in shorter (less than 1–2 decades) time series.

Balance of metabolism

On an annual basis, CR exceeded ^{18}O-GOP by 6 ± 8 mmol O_2 m^{-2} d^{-1}, or approximately 2.3 mol O_2 m^{-2} yr^{-1} (Table 2), a value not statistically different from zero ($p = 0.521$). Such findings imply that the euphotic zone was near metabolic balance over the period of our observations. However, because ^{18}O-GOP decreased more rapidly with depth than CR, we find that heterotrophy prevailed in the deeper portion (75–125 m) of the euphotic zone, with a mean annual deficit of 3.0 ± 1.3 mol O_2 m^{-2} yr^{-1} ($p = 0.006$). Intriguingly, rates of CR were lower during the latter 2019–2020 period of the time series (Fig. 2c; $p = 0.006$), a change that was not accompanied by lower ^{18}O-GOP, resulting in balanced metabolism (^{18}O-GOP = CR) in the deeper 75–125 m layer ($p = 0.791$), and autotrophic conditions (^{18}O-GOP > CR) in the upper 45 m ($p = 0.038$). Variations in the balance between ^{18}O-GOP and CR in our time series were mostly driven by changes in CR and not ^{18}O-GOP (Supporting Information Fig. S10). Net community production values estimated by the difference between 0 and 125 m depth-integrated ^{18}O-GOP and CR were negatively correlated with CR ($p < 0.0001$, $r^2 = 0.603$) but showed no correlation with ^{18}O-GOP ($p = 0.460$) (Supporting Information Fig. S10). The compilation of incubation-based light–dark O_2 measurements presented here (Fig. 5) indicated that on average, CR exceeds GOP ($p < 0.0001$), with an annual deficit of 8 mol O_2 m^{-2} yr^{-1}. These findings are similar to those of Williams et al. (2004). In contrast, numerous non-incubation approaches in the oligotrophic waters of the NPSG have consistently revealed the prevalence of autotrophic conditions (Emerson 2014 and references therein). The discrepancy between incubation and non-incubation approaches might reflect the fact that most of these studies only integrate down to the base of the well-lit mixed layer, while most of the incubation-based methods point to heterotrophy in the dim lower euphotic zone. However, several non-incubation estimates, that have included the lower portion of the euphotic zone, indicate autotrophic conditions prevail in this layer (e.g., Nicholson et al. 2008; Riser and Johnson 2008; Ferrón et al. 2021). The reasons for the discrepancies between incubation and non-incubation based approaches for the determination of NCP in oligotrophic regions remain unresolved (Duarte et al. 2013; Westberry et al. 2012; Williams et al. 2013). Indeed, some studies have shown that incubation-dependent light–dark O_2 methods do not always yield heterotrophic conditions in the oligotrophic gyres; for example, in the low productivity waters of South Atlantic gyre (Serret et al. 2015, 2023). Serret et al. (2023) suggested that large differences in precision and accuracy in existing datasets (e.g., Regaudie-de-Gioux et al. 2014) "may partly explain the sustained disagreements and high uncertainty in regional estimations of NCP based on in vitro changes in O_2."

Our measurements of CR differ from previous measurements of CR in that they are determined as the difference between GOP (measured by the ^{18}O method) and the net daytime change in O_2 inside the bottles. Hence, our CR measurements are derived from daytime incubations under light conditions. In extrapolating daytime measurements to 24-h scale fluxes, we assume that respiration does not substantially change between daytime and nighttime, an assumption that may not be valid for these waters (e.g., Ferrón et al. 2015; Barone et al. 2019). Additionally, our estimates of CR are considered an upper constraint as they include the consumption of newly produced O_2 by water–water reactions (Bender et al. 1999). As a result, the resulting NCP, derived as the difference between ^{18}O-GOP and CR, may be low. In contrast, CR by the light–dark O_2 method is a measurement of the net change in O_2 under dark conditions, typically over a 24-h incubation. For these measurements, respiration is assumed to be the same under dark and light conditions, an assumption that has also been challenged (e.g., Pringault et al. 2007). We find that both estimates of CR were similar (Fig. 5c), while estimates of GOP were not (Fig. 5a). Such findings highlight the challenges in quantifying NCP in oligotrophic environments where net fluxes are many times smaller than GOP and CR. When NCP is derived as the difference between GOP and CR, as done here, small errors associated with either of these fluxes can result in large biases in estimates of NCP. Additionally, given the high day-to-day variability in NCP (e.g., Ferrón et al. 2015), estimates of NCP based on snapshot incubation measurements might not be representative of the mean metabolic state of the system. The measurements reported in this study highlight the need to better characterize not only primary production but also CR as central to improving understanding of variability in the ocean's metabolic balance (Serret et al. 2015, 2023).

Summary and conclusions

The results presented herein show that ^{18}O-GOP at Station ALOHA varies seasonally, with a maximum during summer months and a minimum during the winter. This seasonality is more pronounced than measurements of ^{14}C-PP. Although CR demonstrates similar seasonality to ^{18}O-GOP, it showed substantially more variability. Even though primary production was consistently elevated in the well-lit portion of the euphotic zone, there was greater seasonality in the poorly lit waters of the lower euphotic zone (75–125 m), where primary production was twofold greater in summer than in winter. Our measurements of CR were somewhat more variable than previous measurements based on light–dark O_2 incubations

conducted a decade earlier, but similar in magnitude, while ^{18}O-GOP was on average 32% larger than O_2-GOP. Variability in CR accounted for most of the variance in the balance between ^{18}O-GOP and CR during the study period, highlighting the need to better characterize CR in order to understand changes in the ocean metabolic balance.

Author Contributions

Sara Ferrón: conceptualization (equal), data curation (equal), formal analysis (lead), visualization (lead), writing-original draft preparation (lead), investigation (equal). **Karin M. Björkman:** conceptualization (equal), data curation (equal), investigation (equal), writing-review and editing (equal). **Matthew J. Church:** conceptualization (equal), data curation (equal), investigation (equal), writing-review and editing (equal). **David M. Karl:** conceptualization (equal), investigation (equal), writing-review and editing (equal), funding acquisition (lead).

Acknowledgments

We thank the scientists and technical staff from the HOT program, as well as the field operations team of SCOPE, for their dedicated efforts and their support in facilitating this work. We thank the captains and crew of the RV *Kaimikai-O-Kanaloa*, the RV *Kilo Moana*, and the RV *Falkor* for safe and efficient operations. Additionally, we thank Gerianne Terlouw, Carmen M. Burgos, and Andrés E. Salazar-Estrada for assistance in collecting and analyzing samples; Blake Watkins for Winkler O_2 measurements used to derive metabolic rates by the light–dark O_2 method between 2005 and 2007; Lance Fujieki for HOT data management; and Samuel Wilson, Benedetto Barone, Tara Clemente and HOT chief scientists for their assistance during SCOPE and HOT cruises. We thank Peter J. le B. Williams, Paul Quay, and two anonymous reviewers for helpful comments on the manuscript, and Paul Quay also for providing his published ^{18}O-GOP data. This manuscript has benefited from discussions with members of the SCOR working group 161 ReMO (Respiration in Mesopelagic Ocean). This research was supported by the 2015 Balzan Prize for Oceanography (Premi Balzan, Fondazione Internationale Balzan, Milano, awarded to David M. Karl), the Simons Foundation (SCOPE, awards 329108 and 721252 to David M. Karl and 721221 to Matthew J. Church), the Gordon and Betty Moore Foundation (Grant #3794 to David M. Karl) and the National Science Foundation (OCE-1260164 to Matthew J. Church and OCE-1756517 and EF-0424599 to David M. Karl, and OCE-1911990 to Sara Ferrón).

Conflicts of Interest

None Declared.

References

Barone, B., D. P. Nicholson, S. Ferrón, E. Firing, and D. M. Karl. 2019. "The Estimation of Gross Oxygen Production and Community Respiration from Autonomous Time-Series Measurements in the Oligotrophic Ocean." *Limnology and Oceanography: Methods* 17: 650–664. https://doi.org/10.1002/lom3.10340.

Bender, M. L., J. Orchardo, M.-L. Dickson, R. Barber, and S. Lindley. 1999. "In Vitro O_2 Fluxes Compared with ^{14}C Production and Other Rate Terms during the JGOFS Equatorial Pacific Experiment." *Deep Sea Research Part I* 46: 637–654. https://doi.org/10.1016/S0967-0637(98)00080-6.

Bender, M. L., K. Grande, and K. Johnson. 1987. "A Comparison of Four Methods for Determining Planktonic Community Production." *Limnology and Oceanography* 32: 1085–1098. https://doi.org/10.4319/lo.1987.32.5.1085.

Church, M. J., J. J. Cullen, and D. M. Karl. 2019. "Approaches to Measuring Marine Primary Production." In Encyclopedia of Ocean Sciences, edited by J. K. Cochran, J. H. Bokuniewicz, and L. P. Yager, vol. 1, 3rd ed., 484–492. Amsterdam, the Netherlands: Elsevier. https://doi.org/10.1016/B978-0-12-409548-9.11599-4.

Duarte, C. M., A. Regaudie-de-Gioux, J. M. Arrieta, A. Delgado-Huertas, and S. Agustí. 2013. "The Oligotrophic Ocean Is Heterotrophic." *Annual Review of Marine Science* 5: 551–569. https://doi.org/10.1146/annurev-marine-121211-172337.

Emerson, S. 2014. "Annual Net Community Production and the Biological Carbon Flux in the Ocean." *Global Biogeochemical Cycles* 28: 14–28. https://doi.org/10.1002/2013GB004680.

Ferrón, S., B. Barone, M. J. Church, A. E. White, and D. M. Karl. 2021. "Euphotic Zone Metabolism in the North Pacific Subtropical Gyre Based on Oxygen Dynamics." *Global Biogeochemical Cycles* 35: e2020GB006744. https://doi.org/10.1029/2020GB006744.

Ferrón, S., D. A. del Valle, K. M. Björkman, P. D. Quay, M. J. Church, and D. M. Karl. 2016. "Application of Membrane Inlet Mass Spectrometry to Measure Aquatic Gross Primary Production by the ^{18}O In Vitro Method." *Limnology and Oceanography: Methods* 14: 610–622. https://doi.org/10.1002/lom3.10116.

Ferrón, S., S. T. Wilson, S. Martínez-García, P. D. Quay, and D. M. Karl. 2015. "Metabolic Balance in the Mixed Layer of the Oligotrophic North Pacific Ocean from Diel Changes in O_2/Ar Saturation Ratios." *Geophysical Research Letters* 42: 3421–3430. https://doi.org/10.1002/2015GL063555.

Field, C. B., M. J. Behrenfeld, J. T. Randerson, and P. Falkowski. 1998. "Primary Production of the Biosphere: Integrating Terrestrial and Oceanic Components." *Science* 281: 237–240. https://doi.org/10.1126/science.281.5374.237.

García, H. E., and L. I. Gordon. 1992. "Oxygen Solubility in Seawater: Better Fitting Equations." *Limnology and Oceanography* 37: 1307–1312. https://doi.org/10.4319/lo.1992.37.6.1307.

Halsey, K. H., A. J. Milligan, and M. J. Behrenfeld. 2010. "Physiological Optimization Underlies Growth Rate-Independent Chlorophyll-Specific Gross and Net Primary

Production." *Photosynthesis Research* 103: 125–137. https://doi.org/10.1007/s11120-009-9526-z.

Halsey, K. H., A. J. Milligan, and M. J. Behrenfeld. 2011. "Linking Time-Dependent Carbon-Fixation Efficiencies in *Dunaliella Tertiolecta* (Chlorophyceae) to Underlying Metabolic Pathways." *Journal of Phycology* 47: 66–76. https://doi.org/10.1111/j.1529-8817.2010.00945.x.

Halsey, K. H., R. T. O'Malley, J. R. Graff, A. J. Milligan, and M. J. Behrenfeld. 2013. "A Common Partitioning Strategy for Photosynthetic Products in Evolutionarily Distinct Phytoplankton Species." *The New Phytologist* 198: 1030–1038. https://doi.org/10.1111/nph.12209.

Hamme, R. C., and S. Emerson. 2004. "The Solubility of Neon, Nitrogen and Argon in Distilled Water and Seawater." *Deep Sea Research Part I* 51: 1517–1528. https://doi.org/10.1016/j.dsr.2004.06.009.

Hendricks, M. B., M. L. Bender, and B. A. Barnett. 2004. "Net and Gross O_2 Production in the Southern Ocean from Measurements of Biological O_2 Saturation and its Triple Isotope Composition." *Deep Sea Research Part I* 51: 1541–1561. https://doi.org/10.1016/j.dsr.2004.06.006.

Huang, Y., D. Nicholson, B. Huang, and N. Cassar. 2021. "Global Estimates of Marine Gross Primary Production Based on Machine Learning Upscaling of Field Observations." *Global Biogeochemical Cycles* 35: e2020GB006718. https://doi.org/10.1029/2020GB006718.

IOCCG. 2022. "Ocean Optics and Biogeochemistry Protocols for Satellite Ocean Colour Sensor Validation." In Aquatic Primary Productivity Field Protocols for Satellite Validation and Model Synthesis. (IOCCG Protocols Series), edited by R. A. Vandermeulen and J. E. Chaves, vol. 7, 201. Dartmouth, NS, Canada: International Ocean-Colour Coordinating Group (IOCCG). https://doi.org/10.25607/OBP-1835.

Johnson, K. S., and M. B. Bif. 2021. "Constraint on Net Primary Productivity of the Global Ocean by Argo Oxygen Measurements." *Nature Geoscience* 14: 769–774. https://doi.org/10.1038/S41561-021-00807-Z.

Juranek, L. W., and P. D. Quay. 2005. "In Vitro and In Situ Gross Primary and Net Community Production in the North Pacific Subtropical Gyre Using Labeled and Natural Abundance Isotopes of Dissolved O_2." *Global Biogeochemical Cycles* 19: 1–15. https://doi.org/10.1029/2004GB002384.

Juranek, L. W., and P. D. Quay. 2013. "Using Triple Isotopes of Dissolved Oxygen to Evaluate Global Marine Productivity." *Annual Review of Marine Science* 5: 10.1–10.22. https://doi.org/10.1146/annurev-marine-121211-172430.

Kana, T. M. 1992. "Oxygen Cycling in Cyanobacteria with Specific Reference to Oxygen Protection in *Trichodesmium* Spp." In Marine Pelagic Cyanobacteria: *Trichodesmium* and Other Diazotrophs, edited by J. J. Carpenter, D. G. Capone, and J. G. Rueter, 29–41. Dordrecht, the Netherlands: Springer.

Kana, T. M., C. Darkangelo, M. D. Hunt, J. B. Oldham, G. E. Bennett, and J. C. Cornwell. 1994. "Membrane Inlet Mass Spectrometer for Rapid High-Precision Determination of N_2, O_2, and Ar in Environmental Water Samples." *Analytical Chemistry* 66: 4166–4170. https://doi.org/10.1021/ac00095a009.

Karl, D. M. 2014. "Solar Energy Capture and Transformation in the Sea." *Elementa* 2: 1–6. https://doi.org/10.12952/journal.elementa.000021.

Karl, D. M., and R. Lukas. 1996. "The Hawaii Ocean Time-Series (HOT) Program: Background, Rationale and Field Implementation." *Deep Sea Research Part II: Topical Studies in Oceanography* 43: 129–156. https://doi.org/10.1016/0967-0645(96)00005-7.

Karl, D. M., D. V. Hebel, K. Björkman, and R. M. Letelier. 1998. "The Role of Dissolved Organic Matter Release in the Productivity of the Oligotrophic North Pacific Ocean." *Limnology and Oceanography* 43: 1270–1286. https://doi.org/10.4319/lo.1998.43.6.1270.

Karl, D. M., E. A. Laws, P. Morris, P. J. le B. Williams, and S. Emerson. 2003. "Metabolic Balance of the Open Sea." *Nature* 426: 32. https://doi.org/10.1038/426032a.

Karl, D. M., R. M. Letelier, R. R. Bidigare, et al. 2021. "Seasonal-to-Decadal Scale Variability in Primary Production and Particulate Matter Export at Station ALOHA." *Progress in Oceanography* 195: 102563. https://doi.org/10.1016/j.pocean.2021.102563.

Kiddon, J., M. L. Bender, and J. Marra. 1995. "Production and Respiration in the 1989 North Atlantic Spring Bloom: An Analysis of Irradiance-Dependent Changes." *Deep Sea Research Part I* 42: 553–576. https://doi.org/10.1016/0967-0637(95)00008-T.

Kroopnick, P., and H. Craig. 1972. "Atmospheric Oxygen: Isotopic Composition and Solubility Fractionation." *Science* 175: 54–55. https://doi.org/10.1126/science.175.4017.54.

Laws, E. A., D. G. Redalje, L. W. Haas, et al. 1984. "High Phytoplankton Growth and Production Rates in Oligotrophic Hawaiian Coastal Waters." *Limnology and Oceanography* 29: 1161–1169. https://doi.org/10.4319/lo.1984.29.6.1161.

Laws, E. A., M. R. Landry, R. T. Barber, L. Campbell, M. L. Dickson, and J. Marra. 2000. "Carbon Cycling in Primary Production Bottle Incubations: Inferences from Grazing Experiments and Photosynthetic Studies Using ^{14}C and ^{18}O in the Arabian Sea." *Deep Sea Research Part II: Topical Studies in Oceanography* 47: 1339–1352. https://doi.org/10.1016/S0967-0645(99)00146-0.

Letelier, R. M., A. E. White, R. R. Bidigare, B. Barone, M. J. Church, and D. M. Karl. 2017. "Light Absorption by Phytoplankton in the North Pacific Subtropical Gyre." *Limnology and Oceanography* 62: 1526–1540. https://doi.org/10.1002/lno.10515.

Letelier, R. M., D. M. Karl, M. R. Abbott, and R. R. Bidigare. 2004. "Light Driven Seasonal Patterns of Chlorophyll and Nitrate in the Lower Euphotic Zone of the North Pacific Subtropical Gyre." *Limnology and Oceanography* 49: 508–519. https://doi.org/10.4319/lo.2004.49.2.0508.

Marra, J. 2002. "Approaches to the Measurement of Plankton Production." In Phytoplankton Productivity and Carbon Assimilation in Marine and Freshwater Ecosystems, edited by P. J. le B. Williams, D. R. Thomas, and C. S. Reynolds, 78–108. Oxford, UK: Blackwell.

Marra, J. F., R. T. Barber, and E. Barber. 2021. "A Database of Ocean Primary Productivity from the ^{14}C Method." *Limnology and Oceanography Letters* 6: 107–111. https://doi.org/10.1002/lol2.10175.

Nicholson, D. P., S. Emerson, and C. C. Eriksen. 2008. "Net Community Production in the Deep Euphotic Zone of the Subtropical North Pacific Gyre from Glider Surveys." *Limnology and Oceanography* 53: 2226–2236. https://doi.org/10.4319/lo.2008.53.5_part_2.2226.

Nicholson, D. P., S. T. Wilson, S. C. Doney, and D. M. Karl. 2015. "Quantifying Subtropical North Pacific Gyre Mixed Layer Primary Productivity from Seaglider Observations of Diel Oxygen Cycles." *Geophysical Research Letters* 42: 4032–4039. https://doi.org/10.1002/2015GL063065.

Pei, S., and E. A. Laws. 2013. "Does the ^{14}C Method Estimate Net Photosynthesis? Implications from Batch and Continuous Culture Studies of Marine Phytoplankton." *Deep Sea Research Part I: Oceanographic Research Papers* 82: 1–9. https://doi.org/10.1016/j.dsr.2013.07.011.

Pei, S., and E. A. Laws. 2014. "Does the ^{14}C Method Estimate Net Photosynthesis? II. Implications from Cyclostat Studies of Marine Phytoplankton." *Deep Sea Research Part I* 91: 94–100. https://doi.org/10.1016/j.dsr.2014.05.015.

Pringault, O., V. Tassas, and E. Rochelle-Newall. 2007. "Consequences of Respiration in the Light on the Determination of Production in Pelagic Systems." *Biogeosciences* 4: 105–114. https://doi.org/10.5194/bg-4-105-2007.

Quay, P. D., C. Peacock, K. Björkman, and D. M. Karl. 2010. "Measuring Primary Production Rates in the Ocean: Enigmatic Results Between Incubation and Non-Incubation Methods at Station ALOHA." *Global Biogeochemical Cycles* 24: GB3014. https://doi.org/10.1029/2009GB003665.

Regaudie-de-Gioux, A., S. Lasternas, S. Agustí, and C. M. Duarte. 2014. "Comparing Marine Primary Production Estimates through Different Methods and Development of Conversion Equations." *Frontiers in Marine Science* 1: 135–140. https://doi.org/10.3389/fmars.2014.00019.

Riser, S. C., and K. S. Johnson. 2008. "Net Production of Oxygen in the Subtropical Ocean." *Nature* 451: 323–325. https://doi.org/10.1038/nature06441.

Robinson, C., and P. J. le B. Williams. 2005. "Respiration and its Measurement in Surface Marine Waters." In Respiration in Aquatic Ecosystems, edited by P. A. Del Giorgio and P. J. le B. Williams, 147–180. New York, NY: Oxford University Press.

Serret, P., C. Robinson, M. Aranguren-Gassis, et al. 2015. "Both Respiration and Photosynthesis Determine the Scaling of Plankton Metabolism in the Oligotrophic Ocean." *Nature Communications* 6: 6961. https://doi.org/10.1038/ncomms7961.

Serret, P., J. Lozano, C. B. Harris, et al. 2023. "Respiration, Phytoplankton Size and the Metabolic Balance in the Atlantic Gyres." *Frontiers in Marine Science* 10: 1222895. https://doi.org/10.3389/fmars.2023.1222895.

Stöckel, J., E. A. Welsh, M. Liberton, R. Kunnvakkam, R. Aurora, and H. B. Pakrasi. 2008. "Global Transcriptomic Analysis of *Cyanothece* 51142 Reveals Robust Diurnal Oscillation of Central Metabolic Processes." *Proceedings of the National Academy of Sciences of the United States of America* 105: 6156–6161. https://doi.org/10.1073/pnas.0711068105.

Stoer, A. C., and K. Fennel. 2022. "Estimating Ocean Net Primary Productivity from Daily Cycles of Carbon Biomass Measured by Profiling Floats." *Limnology and Oceanography Letters* 8, no. 2: 368–375. https://doi.org/10.1002/lol2.10295.

Viviani, D. A., D. M. Karl, and M. J. Church. 2015. "Variability in Photosynthetic Production of Dissolved and Particulate Organic Carbon in the North Pacific Subtropical Gyre." *Frontiers in Marine Science* 2: 1–16. https://doi.org/10.3389/fmars.2015.00073.

Westberry, T. K., G. M. Silsbe, and M. J. Behrenfeld. 2023. "Gross and Net Primary Production in the Global Ocean: An Ocean Color Remote Sensing Perspective." *Earth Science Reviews* 237: 104322. https://doi.org/10.1016/j.earscirev.2023.104322.

Westberry, T. K., P. J. le B. Williams, and M. J. Behrenfeld. 2012. "Global Net Community Production and the Putative Net Heterotrophy of the Oligotrophic Oceans." *Global Biogeochemical Cycles* 26: 1–17. https://doi.org/10.1029/2011GB004094.

White, A. E., B. Barone, R. M. Letelier, and D. M. Karl. 2017. "Productivity Diagnosed from the Diel Cycle of Particulate Carbon in the North Pacific Subtropical Gyre." *Geophysical Research Letters* 44: 3752–3760. https://doi.org/10.1002/2016GL071607.

Williams, P. J. le B., P. D. Quay, T. K. Westberry, and M. J. Behrenfeld. 2013. "The Oligotrophic Ocean Is Autotrophic." *Annual Review of Marine Science* 5: 535–549. https://doi.org/10.1146/annurev-marine-121211-172335.

Williams, P. J. le B., P. J. Morris, and D. M. Karl. 2004. "Net Community Production and Metabolic Balance at the Oligotrophic Ocean Site, Station ALOHA." *Deep Sea Research Part I: Oceanographic Research Papers* 51: 1563–1578. https://doi.org/10.1016/j.dsr.2004.07.001.

Wilson, S. T., F. O. Aylward, F. Ribalet, et al. 2017. "Coordinated Regulation of Growth, Activity and Transcription in Natural Populations of the Unicellular Nitrogen-Fixing Cyanobacterium *Crocosphaera*." *Nature Microbiology* 2: 17118. https://doi.org/10.1038/nmicrobiol.2017.118.

Supporting Information

Additional Supporting Information may be found in the online version of this article.

Submitted 07 June 2024
Revised 23 October 2024
Accepted 22 February 2025